Supporting Information

Bi_2WO_6/COF S-scheme heterostructure photocatalyst for H_2O_2 production

Han Liu[a], Jun Zhang[b], Quanlong Xu[c], Hong Tao[a], Tingmin Di[a,*], Quanrong Deng[a,*], Shenggao Wang[a,*]

[a] *Hubei Key Laboratory of Plasma Chemistry and Advanced Materials, School of Materials Science and Engineering, Wuhan Institute of Technology, Wuhan 430205, P. R. China.* Email: ditingmin19@wit.edu.cn, dqrwit@163, Wyysg@163.com.

[b] *Key Laboratory of Green Chemical Process of Ministry of Education, Key Laboratory of Novel Reactor and Green Chemical Technology of Hubei Province, School of Chemical Engineering and Pharmacy, Wuhan Institute of Technology, Wuhan 430205, P. R. China.*

[c] *College of Chemistry and Materials Engineering, Wenzhou University, Wenzhou 325027, PR China.*

1. Characterizations

The surface charge analysis was performed by Zeta potential tester (Nano ZS90, Malvern Zeta sizer, UK). The crystal structure and phase component were investigated by X-ray diffractometer (XRD, Bruker D8 Advance, Germany). Fourier transform infrared (FTIR) spectra were characterized on Nicolet iS50 spectrometers (Thermo Scientific, USA). The morphological results of the photocatalysts were acquired by field emission scanning electron microscopy (FESEM, Gemini SEM 300, Carl Zeiss AG, Germany) equipped with an energy-dispersive X-ray spectrometer (EDS, JED-2300, JEOL, Japan) at 200 kV and transmission electron microscopy (TEM, JEM-F200, Japan). The optical property was analyzed by ultraviolet-visible diffuse reflectance spectra (UV-vis DRS, Shimadzu UV-3600i Plus, Japan). The specific surface area and pore structure of the prepared samples were investigated through nitrogen adsorption–desorption measurements using a nitrogen adsorption apparatus (Quantachrome Autosorb iQ-C, USA). X-ray photoelectron spectra (XPS) were recorded on an electron spectrometer (ESCALAB250XI+, Thermo Fisher, USA) to investigate the surface chemical state of the prepared samples. The photoluminescence (PL) spectroscopy and time-resolved photoluminescence (TRPL) spectra of the samples were analyzed on fluorescence spectrophotometer and fluorescence lifetime spectrophotometer (FLS1000, Edinburgh, UK) with excitation wavelength of 390 nm. Electron paramagnetic resonance (EPR, ELEXSYS IIE 500, Bruker, Germany) was applied to analyze the hydroxyl radicals (·OH) and superoxide radicals ($\cdot O_2^-$), in which 5,5-Dimethyl-1-pyrroline N-oxide (DMPO) was used as trapping agent.

2. Photoelectrochemical measurements

Photoelectrochemical tests were performed on the CHI660C electrochemical workstation with a Pt sheet and Ag/AgCl electrode as the counter electrode and the reference electrode, respectively. The working electrodes were fabricated by doctor blade technique coating photocatalyst on FTO. Na_2SO_4 (0.5 M) was utilized as the electrolyte, a 300 W Xe lamp as light source.

3. Photocatalytic H_2O_2 production experiments

The photocatalytic experiment was carried out in a 100 mL flat-bottomed three-neck flask with a 300 W xenon arc lamp as the light source. In detail, 20 mg of the prepared sample was dispersed to 60 mL aqueous ethanol (10 vol.% ethanol) by ultrasonic. Prior to light irradiation, O_2 was bubbled through the suspension for 30 min to achieve the adsorption/desorption equilibrium of O_2. During illumination, a volume of 1 mL solution was extracted every 15 min and passed through a Millipore filter with a pore size of 0.22 μm to remove the photocatalyst. The amount of H_2O_2 was analyzed by iodometry. Generally, a 200 μL aliquot of the previously obtained solution was transferred into a 5 mL brown centrifuge tube, followed by sequential addition of 800 μL deionized water, 1 mL potassium hydrogen phthalate ($C_8H_5KO_4$, 0.1 mol L^{-1}) aqueous solution, and then 1 mL potassium iodide (KI, 0.4 mol L^{-1}) aqueous solution. After thorough shaking, the mixture was allowed to stand for 30 min. During this process, H_2O_2 reacts with I^- to form I_3^- ($H_2O_2 + 3I^- + 2H^+ \rightarrow I_3^- + 2H_2O$), which exhibits strong absorbance at a wavelength of 350 nm. Consequently, the concentration of I_3^- was determined using a UV-vis spectrometer (UV56CRT, China) in order to estimate the concentration of H_2O_2.

The apparent quantum yields (AQY) of the prepared samples were determined using the same procedure as photocatalytic H_2O_2 production experiments, except that a 300 W Xenon lamp equipped with a 365 nm filter was employed as the light source, allowing only monochromatic light at 365 nm to pass through.

The AQY was calculated according to the following equation:

$$AQY = \frac{2 \times \text{the number of evolved } H_2O_2}{\text{the number of incident photons}} \times 100 \quad (1)$$

The H_2O_2 evolution cycling tests were conducted under the identical procedure of photocatalytic reactions. The reacted photocatalyst in the cycle experiments was centrifuged and rinsed with deionized water for subsequent cycles. The degradation

behavior of H_2O_2 over the as-synthesized photocatalysts was investigated by degrading 1 mmol L^{-1} H_2O_2 under 300 W xenon lamp irradiation.

4. Density function theory (DFT) calculations

All calculations were performed using the CP2K software package for DFT calculations. The functional PBE (Perdew-Burke-Ernzerh) is used to describe the system. The Goedecker-Teter-Hutter (GTH) pseudopotentials and Double-ζ molecularly optimized basis sets (DZVP-MOLOPT-GTH) have been used for all elements. The plane wave energy cutoff is 400 Ry (1 Ry = 13.606 eV). The convergence threshold and convergence criteria of the density matrix are $1*10^{-5}$ Hartree and $4.5*10^{-4}$ Bohr/Hartree, respectively. To eliminate the interaction between the periodic structures of the surface model, the vacuum space is set to 15 Å along the z direction. The van der Waals interaction is modified by using the DFT-D3 method of grime.

5. Nernst's equation

The normal hydrogen electrode potential is:

$$E_{NHE} = E_{Ag/AgCl} + 0.197 + 0.059 \times pH \quad (2)$$

6. Average decay time (τ_{avg})

The average decay lifetime (τ_{avg}) is calculated based on the following equation:

$$\tau_{avg} = \frac{A_1\tau_1^2 + A_2\tau_2^2}{A_1\tau_1 + A_2\tau_2} \quad (3)$$

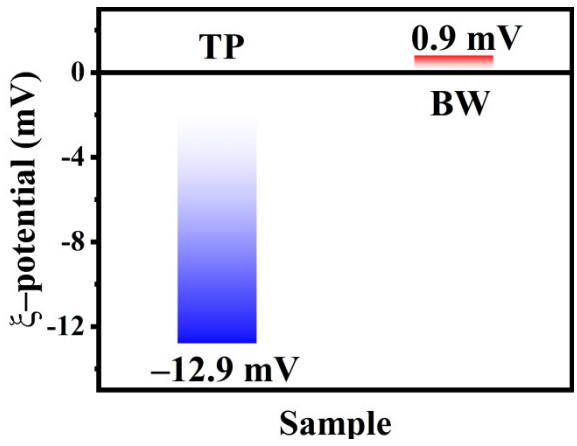

Fig. S1. Zeta potentials of BW and TP samples.

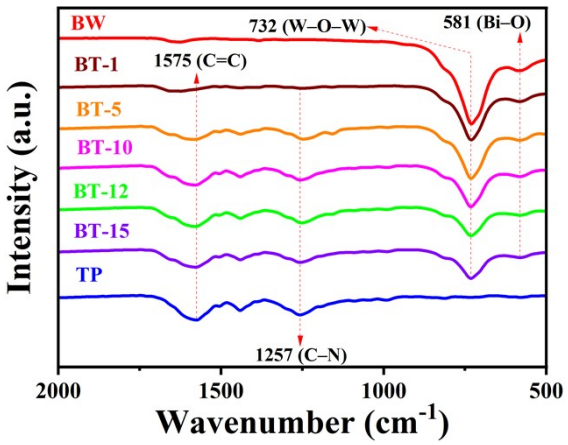

Fig. S2. Enlarged FTIR spectra in the range of 500 ~ 2000 cm^{-1} of BW, TP and BT-X composites.

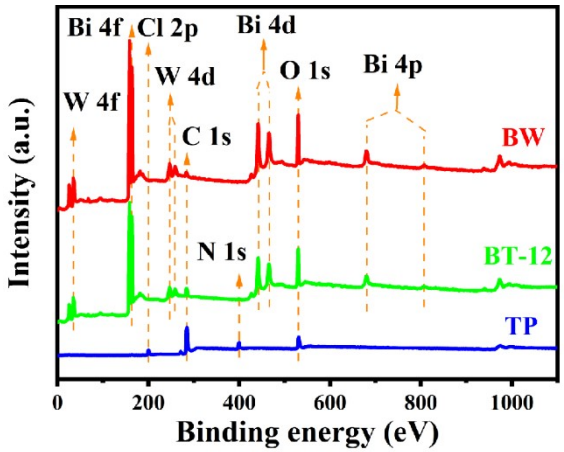

Fig. S3. XPS survey spectra of BW, TP and BT-12 samples.

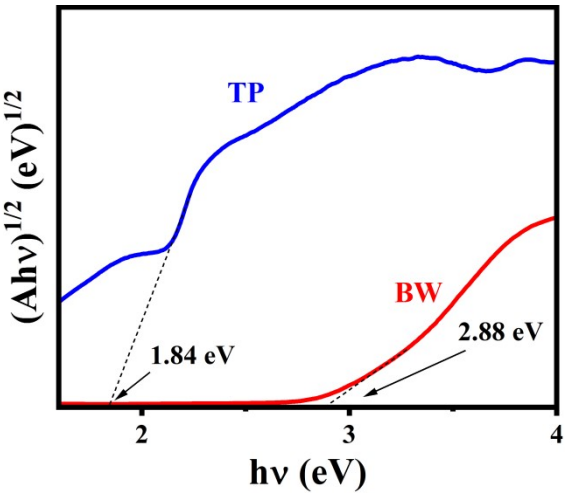

Fig. S4. Tauc plot curves drawn from the UV-vis DRS of BW and TP samples.

Table S1. Comparison of photocatalytic H_2O_2 production activity over the Bi-based and COF-based catalysts.

Photocatalysts	Light source	Scavenger	H_2O_2 yield (μmol L^{-1})	Ref.
PDI-Urea/BiOBr (50 mg)	300 W Xe lamp (λ ≥ 420 nm)	None	23.7	[1]
$MnOOH/BiVO_4/Cu_2O$ (50 mg)	300 W Xe lamp (λ ≥ 420 nm)	PBS	112	[2]
Ag_2CrO_4/Bi_2WO_6 (50 mg)	300 W Xe lamp (λ ≥ 400 nm)	None	19.55	[3]
$CoWO_4@Bi_2WO_6$ (50 mg)	300 W Xe lamp (λ ≥ 420 nm)	None	52.5	[4]
BiOBr/COF (5 mg)	300 W Xe lamp	EtOH	474.3	[5]
$Bi_2S_3@CdS@RGO$ (50 mg)	300 W Xe lamp (λ ≥ 420 nm)	IPA	49.25	[6]
$Bi_2O_2CO_3$/Bi-MOF (20 mg)	300 W Xe lamp	CH_3OH	280.5	[7]
NH_2-MIL-101(Fe)@ MCN/Bi_2O_3 (20 mg)	300 W Xe lamp	None	131.1	[8]
COF/In_2S_3 (15 mg)	300 W Xe lamp (λ ≥ 420 nm)	None	93.3	[9]
Bi_2WO_6/COF (20 mg)	300 W Xe lamp	EtOH	723.0	This work

Table S2. Average lifetimes and fitted parameters of the TRPL decay curves.

Samples	τ_1 (ns)	A_1 (%)	τ_2 (ns)	A_2 (%)	τ_{avg} (ns)
BW	1.59	39.49	20.28	60.51	12.9
TP	0.46	100			0.46
BT-12	0.49	79.01	2.93	20.99	1.00

References

1. W. Wang, X. Li, F. Deng, J. Liu, X. Gao, J. Huang, J. Xu, Z. Feng, Z. Chen and L. Han, *Chinese Chem. Lett.*, 2022, **33**, 5200-5207.
2. J. Huang, H. Shi, X. Wang, P. Wang, F. Chen and H. Yu, *Catal. Sci. Technol.*, 2024, **14**, 2514-2521.

3. T. Xian, W. Jing, L. Di, L. Pan, Y. Zhang, C. Sun, X. Sun, H. Wang and H. Yang, *Appl. Surf. Sci.*, 2025, **682**, 161655.
4. J. Wang, L. Yang and L. Zhang, *Chem. Eng. J.*, 2021, **420**, 127639.
5. H. Zhang, J. Liu, Y. Zhang, B. Cheng, B. Zhu and L. Wang, *J. Mater. Sci. Technol.*, 2023, **166**, 241-249.
6. S. M. Ghoreishian, K. S. Ranjith, B. Park, S.-K. Hwang, R. Hosseini, R. Behjatmanesh-Ardakani, S. M. Pourmortazavi, H. U. Lee, B. Son, S. Mirsadeghi, Y.-K. Han and Y. S. Huh, *Chem. Eng. J.*, 2021, **419**, 129530.
7. J. Wang, Y. Gong, M. Gao, Y. Zheng, Y. Feng, M. Xu, Q. Chu and J. Yan, *ACS Appl. Nano Mater.*, 2023, **7**, 1067-1077.
8. Z. Li, D. Shen, X. Hu, X. Yang, Y. Li and M. Bao, *Chemosphere*, 2023, **343**, 140234.
9. H. Chen, S. Gao, G. Huang, Q. Chen, Y. Gao and J. Bi, *Appl. Catal. B-Environ.*, 2024, **343**, 123545.